

X-ray Diffraction Study of Basal-(*ab*)-Plane Structure and Diffuse Scattering from Silver Atoms in Disordered Stage-2 $\text{Ag}_{0.18}\text{TiS}_2$

BY KEN-ICHI OHSHIMA* AND S. C. MOSS

Department of Physics, University of Houston, Houston, Texas 77004, USA

(Received 7 July 1982; accepted 10 November 1982)

Abstract

X-ray results are presented on the crystallographic parameters in the basal (*ab*) plane and the short-range-order diffuse scattering from intercalated silver atoms in disordered stage-2 $\text{Ag}_{0.18}\text{TiS}_2$ at room temperature. The silver atoms in the intercalated plane occupy the octahedral sites and the in-plane temperature parameter of the silver atoms has a value of $B = 3.0 \pm 0.1 \text{ \AA}^2$, suggesting both weak bonding and correspondingly rapid diffusion. Rodlike diffuse scattering parallel to \mathbf{c}^* at $\frac{1}{3}\frac{1}{3}.0$, $\frac{2}{3}\frac{2}{3}.0$ and their equivalent positions is observed and reveals the two-dimensional (2D) feature of the disordered state. From analyzing this 2D diffuse intensity by the method of Borie & Sparks [*Acta Cryst.* (1971), A27, 198–201], the planar short-range-order parameters were determined. A comparison of this planar short-range order with the 2D Ornstein–Zernike correlation function demonstrates the long-range nature of the 2D short-range order with a correlation range κ^{-1} of $4.88 \pm 0.4 \text{ \AA}$. Using a linearized mean-field approximation for the correlation functions of a binary Ising system well above T_c developed by Clapp & Moss [*Phys. Rev.* (1966), 142, 418–427], a set of oscillatory atomic-pair interaction potential ratios was obtained where the direct interactions were significant out to at least four to five neighbors.

I. Introduction

Interest in intercalated transition-metal dichalcogenides, *i.e.* Li_xTiS_2 (Thompson, 1978; Dahn & Haering, 1981), Ag_xTiS_2 (Scholz & Frindt, 1980; Mori, Ohshima, Moss, Frindt, Plischke & Irwin, 1982), Ag_xTaS_2 (Scholz & Frindt, 1980), has increased recently due to their application as cathodes in high-energy density batteries and also due to their

quasi-two-dimensional (2D) properties. In particular, the structural investigation of intercalated silver atoms between layered TiS_2 sandwiches for stage-2 Ag_xTiS_2 is amenable to straightforward measurement in air and at room temperature, which is well above the proposed ordering temperature of $T_c < 200 \text{ K}$.

Scholz & Frindt (1980) studied the disordered stage-2 $\text{Ag}_{0.20}\text{TiS}_2$ by an X-ray method. They determined that the silver atoms prefer octahedral sites in the basal (*ab*) plane between every two TiS_2 sandwich layers and that there is no change of the host-lattice stacking, *i.e.* the Ag atoms occupy positions in the sulfur van der Waals gap directly between Ti atoms, which are positioned vertically above and below.

More detailed X-ray measurements were performed on the *c*-axis parameters in disordered stage-2 Ag_xTiS_2 ($x = 0.18$ and 0.19) (Mori, Ohshima, Moss, Frindt, Plischke & Irwin, 1982). There it was found that the intercalation of silver ions between sulfur layers produces unequal Ti–S distances in the TiS_2 layer. The charge transfer to the Ti layer induces an expanded Ti–S distance adjacent to the Ag layer. The Ti–S distance away from the Ag ions is accordingly contracted as it presumably becomes more covalent.

In the present paper, we report the result of X-ray measurements on the in-plane structure determination of silver atoms and on the planar pair-correlation or short-range-order (SRO) diffuse scattering from silver in disordered stage-2 $\text{Ag}_{0.18}\text{TiS}_2$ at room temperature.

Generally speaking, the total diffuse scattering contains the above short-range-order component along with static and dynamic displacement terms. The method proposed by Borie & Sparks (1971) for separating this scattering into its individual components has had many successful applications for disordered binary alloy systems (*e.g.* Gragg & Cohen, 1971; Ohshima, Watanabe & Harada, 1976). The present analysis is the first attempt to analyse 2D diffuse scattering intensity using the above separation method. It is an ideal case for the Borie–Sparks method both because of the 2D nature of the diffuse scattering and because one of the binary constituents is a vacancy and thus has zero scattering amplitude.

* On leave from Department of Applied Physics, Nagoya University, Nagoya 464, Japan (present address).

II. Procedures of experiment and analysis

Two Ag_xTiS_2 single crystals were prepared electrolytically by immersing TiS_2 crystals in a 0.1 mol dm^{-3} AgNO_3 solution with Ag metal as the anode (Unger, Reyes, Singh, Curzon, Irwin & Frindt, 1978). Mosaic spreads of these samples parallel to the c axis were about 2° . The size of sample 2, which was used to determine the structure factor in our previous work (Mori, Ohshima, Moss, Frindt, Plischke & Irwin, 1982), was about $1.0 \times 1.0 \times 0.03 \text{ mm}$. The composition of the present sample was determined through an analysis of the $00.L$ Bragg intensities (where capital letters will be used to refer to Bragg peaks) by a least-squares fitting procedure and was determined to be $x = 0.18$. The a_0 and c_0 lattice parameters were 3.419 ± 0.01 and $12.115 \pm 0.003 \text{ \AA}$, respectively. The size of our present sample, which was used to observe the diffuse scattering intensity, was about $4.0 \times 5.0 \times 0.006 \text{ mm}$. The composition of this sample, estimated from the c_0 lattice parameter of $12.115 \pm 0.003 \text{ \AA}$, was again $x = 0.18$.

The X-ray measurements, utilizing both film and counter methods, were performed on a rotating-anode generator (RU-200) operated at maximum 50 kV and 200 mA at room temperature in point-focus geometry. A vertically bent graphite monochromator focused at the counter slit was used to obtain the Mo $K\alpha$ radiation ($\lambda = 0.7107 \text{ \AA}$).

The fixed-crystal-fixed-film technique was used to obtain an X-ray photograph of disordered stage-2 $\text{Ag}_{0.18}\text{TiS}_2$. An exposure time of about one day was required because of the sharp collimation and the thin sample.

To measure quantitatively the X-ray scattered intensities of the sample, a two-circle ($\omega-2\theta$) goniometer was used with manual χ motion. The horizontal and vertical divergences of the beam were 0.5 and 0.6° , respectively. The beam size at the counter slit was $0.8 \times 1.2 \text{ mm}$. The $\lambda/2$ component from the monochromator was eliminated using a single-channel pulse-height analyzer together with a scintillation detector. A transmission method was used to measure $HO.L$ and $HH.L$ Bragg reflections for sample 2 as well as the diffuse scattering on the $(HK.0)$ plane and along the $\langle HK.L \rangle$ direction for our present sample, where H , K and L are integers. The stability of the incident beam was better than 4%.

To convert the measured diffuse intensity into absolute units, direct beam power was determined by measuring and analyzing the $00.L$ Bragg reflections of our crystal ($20 \leq L \leq 29$), where the former reflection method was employed (Mori, Ohshima, Moss, Frindt, Plischke & Irwin, 1982). This incident power could thereby be estimated as $(2.1 \pm 0.1) \times 10^7 \text{ photons s}^{-1}$. Air scattering and the counter noise were eliminated by measuring the intensity without the sample. The

absorption parameter μt is sufficiently small for this sample ($\mu = 0.04$) so that this method provides an effective correction. The fluorescent radiation from the sample was neglected in our analysis. The contribution from Compton scattering was also eliminated from the intensity data after the above conversion to absolute units, using the calculated values (Cromer & Mann, 1967; Cromer, 1969). The dispersion correction for the silver atomic scattering factor (*International Tables for X-ray Crystallography*, 1974) and the usual transmission absorption correction were applied to the data. The diffuse intensity in the vicinity of Brillouin zone centers (Bragg peaks) was obtained by smooth extrapolation of the intensity in regions away from zone centers.

We shall treat the present diffuse scattering, originating from correlations among intercalated silver atoms in the basal (ab) plane, as purely 2D scattering, because the so-called 'correlation length' parallel to the c axis between silver-atom planes was very short ($\sim 2.4 \text{ \AA}$) in comparison with the nearest-neighbor silver-plane separation ($\sim 12 \text{ \AA}$) as described in the next section. The resulting 2D diffuse scattering can then be written as the sum of three terms (Borie & Sparks, 1971):

$$I_D' = I_D / [NX_{\text{Ag}}(1 - X_{\text{Ag}})f_{\text{Ag}}^2] = I^{\text{SRO}} + I^{\text{SE}} + I^{\text{TDS+H}}, \quad (1)$$

where I^{SRO} is the scattering due to SRO, I^{SE} the size-effect-modulation term and $I^{\text{TDS+H}}$ the contribution from thermal diffuse and Huang scattering which both peak at the zone centers. N , X_{Ag} and f_{Ag} are the number of atoms irradiated, the composition of silver atoms in silver layers and the scattering factor for the silver atom (including an average or effective temperature factor), respectively. Each term in (1) is given as a series:

$$I^{\text{SRO}} = \sum_l \sum_m \alpha_{lm} \cos 2\pi(h_1 l + h_2 m), \quad (2)$$

$$I^{\text{SE}} = -\sum_l \sum_m (h_1 \gamma_{lm}^x + h_2 \gamma_{lm}^y) \sin 2\pi(h_1 l + h_2 m), \quad (3)$$

$$I^{\text{TDS+H}} = \sum_l \sum_m (h_1^2 \delta_{lm}^x + h_2^2 \delta_{lm}^y + h_1 h_2 \epsilon_{lm}^{xy}) \times \cos 2\pi(h_1 l + h_2 m). \quad (4)$$

The integers l and m define a lattice site according to the relation

$$\mathbf{r}_{lm} = l\mathbf{a} + m\mathbf{b},$$

where \mathbf{a} and \mathbf{b} are translation vectors of the average (Ti) hexagonal cell, and h_1 and h_2 (and h_3 , along \mathbf{c}^*) are the continuous coordinates in the hexagonal reciprocal space.

α_{lm} is a 2D SRO parameter defined by

$$\alpha_{lm} = 1 - P_{lm}^{\text{Ag}^2} / (1 - X_{\text{Ag}}), \quad (5)$$

where $P_{lm}^{Ag\Box}$ is the probability of finding a vacant atom (\Box) at the end of a vector \mathbf{r}_{lm} when the origin is occupied by a silver atom. Other Fourier coefficients are given by

$$\gamma_{lm}^x = -2\pi\{[X_{Ag}/(1 - X_{Ag}) + \alpha_{lm}] \langle x_{lm}^{AgAg} \rangle\} \quad (6)$$

$$\delta_{lm}^x = 4\pi^2\{[X_{Ag}/(1 - X_{Ag}) + \alpha_{lm}] \langle (x_{lm}^{AgAg})^2 \rangle\} \quad (7)$$

$$\epsilon_{lm}^{xy} = 8\pi^2\{[X_{Ag}/(1 - X_{Ag}) + \alpha_{lm}] \langle x_{lm}^{AgAg} y_{lm}^{AgAg} \rangle\}. \quad (8)$$

The quantity $\langle x_{lm}^{AgAg} \rangle$ describes the average displacement along the $[10.0]$ axis between an Ag–Ag atom pair separated by the vector \mathbf{r}_{lm} with similar definitions for the quantities $\langle (x_{lm}^{AgAg})^2 \rangle$ and $\langle (x_{lm}^{AgAg} y_{lm}^{AgAg}) \rangle$. γ_{lm}^x , δ_{lm}^x and ϵ_{lm}^{xy} in (6) through (8) do not contain the ratios of atomic scattering factors, $f_A/(f_A - f_B)$ and $f_B/(f_A - f_B)$, because one constituent atom of our sample is a vacancy. In the usual case of a disordered binary alloy, these ratios of atomic scattering factors considerably complicate the analysis of the diffuse scattering (Tibbals, 1975). In this experiment, the diffuse intensity at about 2300 points in reciprocal space over the area of two full unit cells was measured, and the above-described method was employed to separate the observed intensity into its component features.

III. Results

1. Crystallographic parameters of the basal (*ab*) plane

Three series of *HO.L* and *HH.L* Bragg reflections were measured and analyzed to determine both the temperature parameters of each atom parallel to the basal (*ab*) plane using the former procedure (Mori, Ohshima, Moss, Frindt, Plischke & Irwin, 1982) and also the average structure of the silver atoms in the intercalated plane, *i.e.* whether they are positioned at the octahedral sites, *i.e.* whether they are positioned at the octahedral sites as proposed by Scholz & Frindt (1980). As shown in Table 1, the temperature parameter of the silver atom, $B_{Ag} = 3.0 \text{ \AA}^2$, has a particularly large value compared with that of the titanium and sulfur atoms with a root-mean-square displacement of the silver atom equal to 0.19 \AA . This clearly suggests that the vibration of the silver atom at the average lattice site in the intercalated plane is large and indicates both weak bonding and correspondingly rapid planar diffusion as well as possibly large static displacements of Ag from the average lattice sites as defined by the lattice parameter. The temperature

parameters for pure TiS_2 are compared in Table 1 (Chianelli, Scanlon & Thompson, 1975). There are not large differences between B_{Ti} and B_S in pure TiS_2 or disordered stage-2 $\text{Ag}_{0.18}\text{TiS}_2$. The Ag vibration perpendicular to the basal plane was also quite normal in disordered stage-2 $\text{Ag}_{0.18}\text{TiS}_2$ (Mori, Ohshima, Moss, Frindt, Plischke & Irwin, 1982).

2. Diffuse scattering from silver atoms in the basal plane

In § III.1, we determined both the temperature parameters and the average structure of the silver atoms in the basal plane. Based on these experimental results, we performed the following study of the diffuse scattering from disordered stage-2 $\text{Ag}_{0.18}\text{TiS}_2$ assuming it to be a disordered Ising-like lattice gas of approximate planar concentration, $X_{Ag} \approx \frac{1}{3}$.

Fig. 2 shows the monochromatic X-ray diffraction pattern of our present sample, taken with the fixed-crystal–fixed-film technique. The \mathbf{c}^* direction is perpendicular to this figure. The Ewald sphere ($1/\lambda = 1.407 \text{ \AA}^{-1}$) has barely been intersected at 20.1, 02.1

Table 1. Temperature parameters of constituent atoms in disordered stage-2 $\text{Ag}_{0.18}\text{TiS}_2$ and pure TiS_2 parallel to the basal (*ab*) plane

The temperature parameters for pure TiS_2 were determined by Chianelli, Scanlon & Thompson (1975).

	$B_S (\text{\AA}^2)$	$B_{Ti} (\text{\AA}^2)$	$B_{Ag} (\text{\AA}^2)$
Stage-2 $\text{Ag}_{0.18}\text{TiS}_2$	1.08 (± 0.13)	1.18 (± 0.14)	3.00 (± 0.10)
Pure TiS_2	1.00 (± 0.02)	0.76 (± 0.02)	—

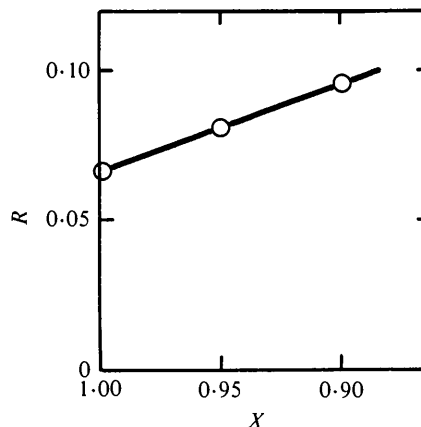


Fig. 1. *R* factor vs the fraction of the silver atoms occupying octahedral sites *X*. The *R* factor is given as $R = \frac{\sum_i |F_{obs}(i)| - |F_{calc}(i)|}{\sum_i |F_{obs}(i)|}$. The structure factor $F_{calc}(i)$ is assumed to be $|F_{calc}(i)| = [X|F_{calc}^{oct}|^2 + (1 - X)|F_{calc}^{tet}|^2]^{1/2}$, where F_{calc}^{oct} and F_{calc}^{tet} refer to the structure factors for the silver atoms in the octahedral sites and tetrahedral sites respectively. Both detailed formulae are in Appendix I.

and their equivalent Laue spots. At 10.0, 01.0, 11.0 and the equivalent spots, the Ewald sphere was not crossed, but tails of these reflections can be observed because of a large mosaic spread and thermal diffuse scattering. Rodlike diffuse scattering parallel to \mathbf{c}^* at $\frac{1}{2}\frac{1}{2}.h_3$, $\frac{2}{3}\frac{2}{3}.h_3$ and their equivalent positions are observed, where h_3 assumes non-integer values along \mathbf{c}^* .

These diffuse intensity distributions parallel to the \mathbf{c}^* direction and centered at $h_3 = 0$, $\frac{2}{3}\frac{2}{3}.0$ and $\frac{1}{2}\frac{1}{2}.0$, were measured and are shown in Fig. 3 in arbitrary units. Both Figs. 2 and 3 verify our assignment of disordered lattice gas to this system. The insert shows the schematic intensity distribution for the $(h_1h_2.h_3)$ reciprocal plane. The so-called 'correlation length' was estimated from the inverse half-width at half-maximum. The average value, 2.38 Å, is about $\frac{1}{2}$ of the silver-plane separation of 12.115 Å, and verifies essentially the 2D feature of diffuse scattering from this sample. The fall off in Fig. 3 is thus due essentially to the form factor for a single layer of intercalated silver atoms. It is not, however, straightforward to convert this functional dependence directly into a planar c -axis electron density. Further work is in progress on this issue.

Fig. 4(a) shows the total diffuse intensity distribution I_D observed on the $(h_1h_2.0)$ reciprocal-lattice plane in absolute units, where the contributions from the Compton scattering and background have been subtracted as described in § II. The intensity distribution due to SRO diffuse scattering was separated

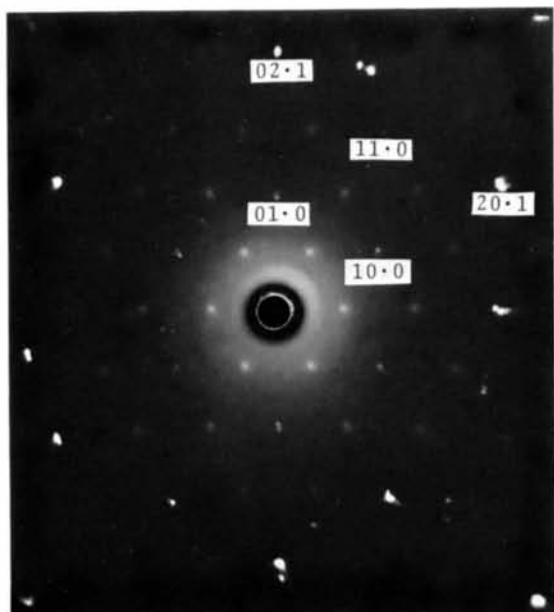


Fig. 2. The monochromatic X-ray diffraction pattern of the present sample taken with the fixed-crystal-fixed-film technique. The \mathbf{c}^* direction is perpendicular to this photograph. The exposure time was about one day at 50 kV and 200 mA.

from the total diffuse intensity in Fig. 4(a) using the separation method described in (1) through (4) and is shown in Fig. 4(b). This SRO diffuse scattering appears to have nearly cylindrical symmetry. By performing the Fourier inversion of I^{SRO} [(2)], 2D SRO parameters, α_i , were determined and are given in Table 2 where the suffix i denotes the shell number. The value of 0.973 obtained for α_0 is close to 1.0 as theoretically required although this may be a somewhat fortuitous result of background subtraction. Ratios of the deviation from the SRO parameters for the perfectly ordered structure (α_i^0), α_i/α_i^0 , were calculated to compare with the 2D Ornstein-Zernike correlation function (Fisher, 1962). In this calculation, we assumed that at low temperature the $\sqrt{3} \times \sqrt{3} R30^\circ$ 2D ordering of silver atoms in an intercalated plane will occur. For the stoichiometric composition, the values of α_i^0 are $-\frac{1}{2}$ and 1 with dependence on i . The α_i^0 parameters corresponding to the composition of the present sample are estimated to

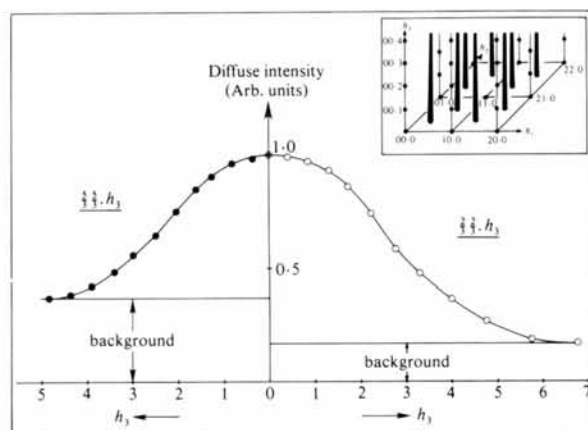


Fig. 3. Diffuse intensity distribution parallel to the \mathbf{c}^* (or h_3) direction centered on $\frac{2}{3}\frac{2}{3}.0$ and $\frac{1}{2}\frac{1}{2}.0$ in arbitrary units. The insert shows the schematic intensity distribution for the $(h_1h_2.h_3)$ reciprocal plane (the \mathbf{c}^* dependence). The flat tops of outer rods are due simply to truncation effects.

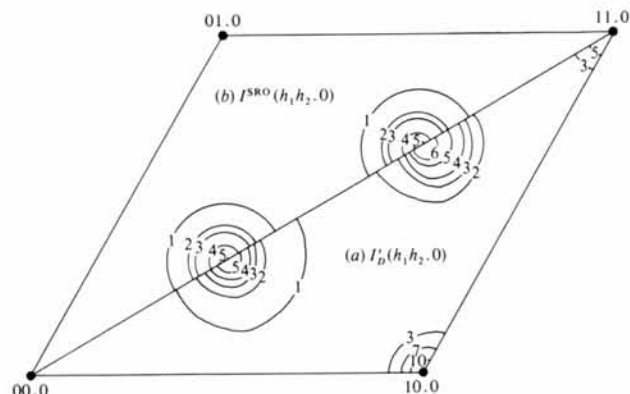


Fig. 4. Intensity distribution in $(h_1h_2.0)$ plane of reciprocal space in absolute units. (a) Total diffuse intensity. (b) SRO component of the total diffuse scattering.

be -0.445 and 0.890 provided that the excess silver atoms distribute randomly over the vacant sites in the ordered plane and do not fill domain boundaries in a non-random fashion. The Ornstein-Zernike function for the 2D case is given as

$$|\alpha(r)/\alpha^0(r)| = A \frac{e^{-\kappa r}}{r^{1/2}} \left\{ 1 + \theta\left(\frac{-1}{\kappa r}\right) \right\}, \quad (9)$$

where A is a normalization constant, r is the distance from the origin and $1/\kappa$ is the correlation length. $\theta(-1/\kappa r)$, which refers to correction of order $1/\kappa r$, was neglected because the Ornstein-Zernike formula is asymptotic for large r in any case. Two adjustable parameters A and $1/\kappa$ were determined using a least-squares-fitting procedure. As shown in Fig. 5, the smooth curve represents the asymptotic behavior expected for large r' and gives an excellent fit for $r' \geq 2.7$, where r' is equal to r/a_0 . The correlation length $1/\kappa$ is 4.88 ± 0.35 Å. The long-range nature of the SRO is quite evident. It is also clear that the direction of the neglected correction of order $(-1/\kappa r)$ will improve the fit at smaller r' ; the inclusion of a

smaller temperature parameter for near neighbors than for distant neighbors (Walker & Keating, 1961) will, however, make the fit worse at small r' !

In a linearized mean-field approximation for the correlation function of a binary Ising system, developed by Clapp & Moss (1966), the SRO diffuse scattering intensity is expressed by

$$I^{\text{SRO}}(\mathbf{k}) = C / \left\{ 1 - \frac{T_c}{T} \frac{V(\mathbf{k})}{V(\mathbf{k}_m)} \right\}, \quad (10)$$

where $V(\mathbf{k})$ is a Fourier transform of the pair-interaction potential given as

$$V(\mathbf{r}) = \frac{1}{2} \{ V^{\text{A8A8}}(\mathbf{r}) + V^{\square\square}(\mathbf{r}) - 2V^{\text{A8}\square}(\mathbf{r}) \} \quad (11)$$

between pairs of atoms separated by a vector \mathbf{r} . The mark \square , as before, means a vacancy. $V(\mathbf{k}_m)$ is the minimum value of $V(\mathbf{k})$ at $\mathbf{k} = \mathbf{k}_m$, where \mathbf{k}_m often corresponds to a superlattice point in the ordered reciprocal space. T_c is the critical temperature and C is a normalization constant. This expression has been particularly successful well above T_c in evaluating ratios of interaction energies (Moss & Clapp, 1968; Mozer, Keating & Moss, 1968).

From (10), 2D atomic pair-interaction potential ratios were determined using a former procedure (Ohshima, Watanabe & Harada, 1976) and are shown in Fig. 6. To estimate the accuracy of the pair-interaction-potential ratios, the SRO parameters α_i^{syn} were synthesized and compared with α_i . The reliability factor

$$R = \frac{\sum_{i \neq 0} |\alpha_i - \alpha_i^{\text{syn}}|}{\sum_{i \neq 0} |\alpha_i|} \quad (12)$$

was estimated to be 0.15 , which is considered reasonable, as discussed in the next section. In this calculation, the normalized relation

$$\sum_{i \neq 0} |\alpha_i| = \sum_{i \neq 0} |\alpha_i^{\text{syn}}|$$

was used. As shown in Fig. 6, the direct pair-interaction potential is long range and oscillatory.

This pair potential was compared with the free-electron screening model for pair interactions between

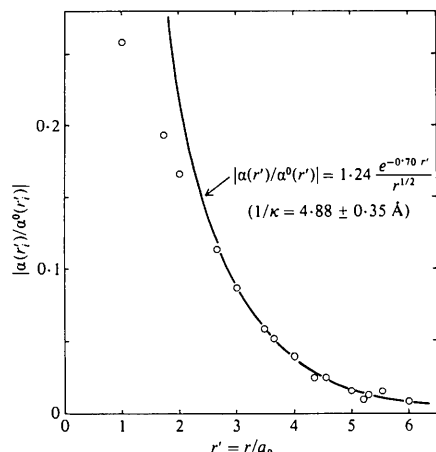


Fig. 5. The values $|\alpha(r'_i)/\alpha^0(r'_i)|$ vs the normalized interatomic distance $r' \equiv r_i/a_0$. $\alpha^0(r'_i)$ is the SRO parameter for the perfectly ordered $\sqrt{3} \times \sqrt{3}$ R30° structure. The smooth curve was calculated from the 2D Ornstein-Zernike correlation function using a least-squares-fitting method. It is difficult to estimate the actual error bars, but $\alpha(r_1)$ and $\alpha(r_2)$ are particularly sensitive to background extrapolation under Bragg peaks and thermal correction.

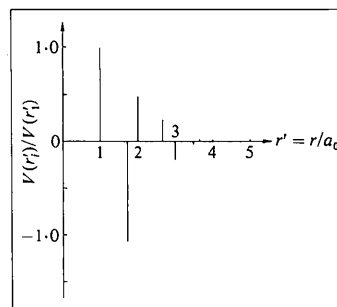


Fig. 6. Atomic-pair interaction ratio $V(r'_i)/V(r'_1)$ vs r' where $V(r'_i)$ is given by (11) of the text.

atoms. According to Roth, Zeiger & Kaplan (1966) and Krivoglaz (1969), the ratio of the 2D pair-interaction potentials at large distances is given as

$$V(r_i)/V(r_1) = A \frac{\sin(2k_F a_0 r_i + \varphi)}{r_i^2}, \quad (13)$$

where k_F is the Fermi wave vector, φ a phase factor and A a constant. The quantity $k_F a_0$ is related to the electron/atom ratio (e/a) and given as $1.55 (e/a)^{1/2}$. In the present case, the e/a value was calculated to be 0.36 from the composition based simply on the silver concentration, assuming the number of conduction electrons to be one for a silver atom. An attempt was made to fit (12) to the present result by adjusting two parameters A and φ . However, it was not possible to find a screening curve which fits well all the potential values. Part of the disagreement may be ascribed to be a non-circular shape of the Fermi surface. In addition, it must be pointed out that the conduction electrons are contributed (donated) mainly to the Ti in the TiS_2 layers and therefore the screening problem is considerably more complicated than we have assumed. Nevertheless, it seems likely that the Fermi surface parameters of the quasi 2D $\text{Ag}_{0.18}\text{TiS}_2$ metallic system are crucial in the screening of the Ag intercalant and the determination of the Ag–Ag interaction.

IV. Discussion

1. Accuracy of Fourier coefficients

As pointed out by Gragg, Hayakawa & Cohen (1973), there are several sources of error that occur in obtaining Fourier coefficients from the total diffuse scattering.

In our case, there is no problem about the variation of ratios of the atomic scattering factor with scattering angle as described in § II. There is, however, a difficulty in estimating the constant background near the Brillouin zone center. Various trials to obtain SRO parameters through changing the background were performed. We have concluded that only α_1 and α_2 are influenced through this change, which, however, produces a large possible error in R of (12). Therefore, it can be stated that the Ornstein–Zernike function estimated in § III.2 is essentially independent of the background level, which is not surprising because $I^{\text{SRO}}(\mathbf{k})$ is poorly determined in the wings but well determined in the vicinity of the superlattice positions.

It is difficult to obtain other Fourier coefficients γ_{lm}^x , δ_{lm}^x and ϵ_{lm}^{xy} [(6) through (8)] because one can never completely eliminate the contribution from the fundamental reflections near the Brillouin zone center without much better resolution. But we obtained rough values of γ_{lm}^x , with an error estimate of about 100%. As

seen in (6), it is possible to recover $\langle x_{lm}^{\text{AgAg}} \rangle$ directly. Fig. 7 shows the orientation direction of the average displacement of silver atoms when an origin is occupied by a silver atom. From this figure, we can deduce that the displacement of silver atoms which occupy the first-nearest-neighbor $\sqrt{3} \times \sqrt{3} R30^\circ$ 2D ordered lattice points is expansive while the second-neighbor occupancy is contractive. It may qualitatively be said that these elastic displacements favor the $\sqrt{3} \times \sqrt{3} R30^\circ$ 2D ordering. Certainly Fig. 7 provides evidence for disordered-basal-plane expansion on intercalation (Scholz & Frindt, 1980; Mori, Ohshima, Moss, Frindt, Plichke & Irwin, 1982).

2. Stability of the 2D ordered structure

We can calculate the configurational energy for the ordered state, given as

$$E = 2X_A \sum_j Z_j \{P_{AA}(r_j) - X_A\} V(r_j), \quad (14)$$

where X_A is the composition of A atoms, Z_j the j th coordination number, $P_{AA}(r_j)$ a probability of finding A – A atomic pairs between the interatomic distance r_j and $V(r_j)$ the pair-interaction-potential energy given as (11).

If $\sqrt{3} \times \sqrt{3} R30^\circ$ 2D ordering of silver atoms in an intercalated plane occurs, E is expressed as

$$E = -\frac{4}{3}V(r_1) \{1 + V(r_3)/V(r_1) + 2V(r_4)/V(r_1)\} \quad (15)$$

up to the fifth-nearest neighbor at the stoichiometric composition. But, the composition of the present sample is not exactly stoichiometric and (15) must be slightly modified. The modified relation is given as the following equation

$$E = -1.322V(r_1) \{1 - 0.004V(r_2)/V(r_1) + V(r_3)/V(r_1) + 2V(r_4)/V(r_1) - 0.004V(r_5)/V(r_1)\}. \quad (16)$$

Introducing our experimental data into (16), we find $E \simeq -2.6V(r_1)$. As it is thought that the sign of $V(r_1)$ must physically be positive, E has a negative sign.

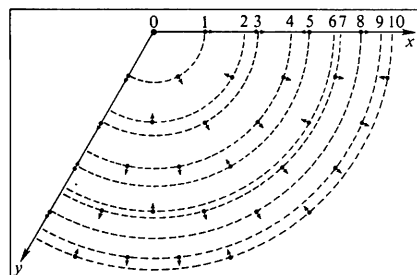


Fig. 7. Orientation direction of the average displacement of silver atoms when an origin site, 0, is occupied by a silver atom. 1, 2, 3, ... refer to the coordination-shell numbers.

Clearly the stability region of the ordered phase is observed for our data. No detailed structure analysis of the ordered phase has been done to date. It is felt that the actual ordered structure may be more complicated than the idealized $\sqrt{3} \times \sqrt{3}$ $R30^\circ$ 2D ordering of silver atoms in an intercalated plane, especially as three-dimensional effects intervene and the aforementioned domain pinning seems to persist. By this we mean that, as Suter, Shafer, Horn & Dimon (1982) have also indicated in stage-1 crystals, it is quite difficult to affect ordering, in the sense of sharp superlattice peaks, on cooling a non-stoichiometric crystal. Those authors find, however, that as stoichiometry is approached the superlattice peaks sharpen, *i.e.* the residual broadening is not a kinetic effect due to sluggish diffusion.

V. Summary and conclusion

In summary, the present X-ray study of disordered stage-2 $\text{Ag}_{0.18}\text{TiS}_2$ shows that:

(a) the silver atoms in the intercalated plane occupy the octahedral sites and the in-plane temperature parameter of the silver atoms has a large value indicating both weak bonding and correspondingly rapid diffusion along with possible static effects;

(b) rodlike diffuse scattering parallel to \mathbf{c}^* , observed at $\frac{1}{3}\frac{1}{3}.0$, $\frac{2}{3}\frac{2}{3}.0$ and their equivalent positions shows a 2D feature, suggesting that a disordered 2D lattice gas is appropriate to this system;

(c) the 2D Ornstein–Zernike correlation function can be fitted to the planar short-range-order parameters evaluated experimentally using the Borie–Sparks method; and

(d) the long-range oscillating 2D atomic-pair interaction potential ratios were obtained based on a linearized mean-field approximation for the correlation functions.

We thank Professor J. C. Irwin of Simon Fraser University for preparing the specimens and for helpful discussions. M. Mori performed some of the preliminary measurements of the scattering discussed here and we thank him, as well, for helpful comments.

This research was supported partly through a joint Michigan State University–USARO project on intercalation compounds at the University of Houston. K. Ohshima has been supported by the US Department of Energy under contract DE-AS05-76ERO5111,

APPENDIX I

The structure factors of disordered stage-2 Ag_xTiS_2 when the silver atoms occupy the octahedral or tetrahedral sites are given as

$$F_{\text{calc}}^{\text{oct}} = 2(-1)^L (x f_{\text{Ag}} + f_{\text{Ti}} \cos 2\pi z L) + f_{\text{S}}(-1)^{H+K} \{ \cos 2\pi[\frac{1}{6}(H-K) - (z-y_2)L] + \cos 2\pi[\frac{1}{6}(H-K) + (z+y_1)L] \} \quad (A1)$$

and

$$F_{\text{calc}}^{\text{tet}} = 2(-1)^L (x f_{\text{Ag}} \{ \cos 2\pi(H/3 + \frac{2}{3}K) + i \sin 2\pi(H/3 + \frac{2}{3}K) \} + f_{\text{Ti}} \cos 2\pi z L + f_{\text{S}}(-1)^{H+K} \{ \cos 2\pi[\frac{1}{6}(H-K) - (z-y_2)L] + \cos 2\pi[\frac{1}{6}(H-K) + (z+y_1)L] \}) \quad (A2)$$

H , K and L are the Miller indices. Distance parameters z , y_1 and y_2 have the same meaning as in our previous paper (Mori, Ohshima, Moss, Frindt, Plischke & Irwin, 1982). f_{Ag} , f_{Ti} , and f_{S} are the scattering amplitudes, including thermal effects, of Ag, Ti and S atoms. x is the atom fraction of Ag. The atomic scattering factor of atom n , f_n , is expressed as

$$f_n = f_n^0 \exp\{-B_n(\sin \theta/\lambda)^2\}, \quad (A3)$$

where f_n^0 is the tabulated scattering factor of atom n (including dispersion) and $B_n = 8\pi^2 \langle u^2 \rangle_n$. $\langle u^2 \rangle_n$ is the mean-square atomic displacement and is equal to $\langle u_{ab}^2 \rangle_n \sin^2 \delta + \langle u_c^2 \rangle_n \cos^2 \delta$. $\langle u_{ab}^2 \rangle_n$ and $\langle u_c^2 \rangle_n$ are the mean-square components parallel and perpendicular to the basal (*ab*) plane and δ is the angle between the diffraction vector and the c axis.

To check whether the silver atoms in the intercalated plane are positioned at the octahedral or tetrahedral sites, the structure factor $F_{\text{calc}}(i)$ is assumed as

$$|F_{\text{calc}}(i)| = [X|F_{\text{calc}}^{\text{oct}}|^2 + (1-X)|F_{\text{calc}}^{\text{tet}}|^2]^{1/2}, \quad (A4)$$

where X is the fraction of the silver atoms occupying octahedral sites.

We have already determined both the distance parameters z , y_1 and y_2 and the temperature parameters of Ag, Ti and S atoms parallel to the c axis, given in Table 1 in our previous paper (Mori, Ohshima, Moss, Frindt, Plischke & Irwin, 1982). Those values were used in calculating the structure factor $F_{\text{calc}}(i)$.

References

- BORIE, B. & SPARKS, C. J. (1971). *Acta Cryst.* **A27**, 198–201.
- CHIANELLI, R. R., SCANLON, J. C. & THOMPSON, A. H. (1975). *Mater. Res. Bull.* **10**, 1379–1382.
- CLAPP, P. C. & MOSS, S. C. (1966). *Phys. Rev.* **142**, 418–427.
- CROMER, D. T. (1969). *J. Chem. Phys.* **50**, 4857–4859.
- CROMER, D. T. & MANN, J. B. (1967). *J. Chem. Phys.* **47**, 1892–1893.
- DAHN, J. R. & HAERING, R. R. (1981). *Solid State Commun.* **40**, 245–248.
- FISHER, M. E. (1962). *Physica (Utrecht)*, **28**, 172–180.
- GRAGG, J. E. JR & COHEN, J. B. (1971). *Acta Metall.* **19**, 507–519.
- GRAGG, J. E. JR, HAYAKAWA, M. & COHEN, J. B. (1973). *J. Appl. Cryst.* **6**, 59–66.
- International Tables for X-ray Crystallography* (1974). Vol. IV. Birmingham: Kynoch Press.
- KRIVOGLAZ, M. A. (1969). *Theory of X-ray and Thermal Neutron Scattering by Real Crystals*. New York: Plenum.
- MORI, M., OHSHIMA, K., MOSS, S. C., FRINDT, R. F., PLISCHKE, M. & IRWIN, J. C. (1982). *Solid State Commun.* **43**, 781–784.

- MOSS, S. C. & CLAPP, P. C. (1968). *Phys. Rev.* **171**, 764–777.
 MOZER, B., KEATING, D. T. & MOSS, S. C. (1968). *Phys. Rev.* **175**, 868–876.
 OHSHIMA, K., WATANABE, D. & HARADA, J. (1976). *Acta Cryst.* **A32**, 883–892.
 ROTH, L. M., ZEIGER, H. J. & KAPLAN, T. A. (1966). *Phys. Rev.* **149**, 519–525.
 SCHOLZ, G. A. & FRINDT, R. F. (1980). *Mater. Res. Bull.* **15**, 1703–1716.
 SUTER, R. M., SHAFER, M. W., HORN, P. M. & DIMON, P. (1982). *Phys. Rev. B*, **26**, 1495–1498.
 THOMPSON, A. H. (1978). *Phys. Rev. Lett.* **40**, 1511–1514.
 TIBBALS, J. E. (1975). *J. Appl. Cryst.* **8**, 111–114.
 UNGER, W. K., REYES, J. M., SINGH, O., CURZON, A. E., IRWIN, J. C. & FRINDT, R. F. (1978). *Solid State Commun.* **28**, 109–112.
 WALKER, C. B. & KEATING, D. T. (1961). *Acta Cryst.* **14**, 1170–1176.

Acta Cryst. (1983). **A39**, 305–310

Secondary Extinction Factor for Spherical Crystals

BY T. KAWAMURA AND N. KATO

Department of Crystalline Materials Science, Faculty of Engineering, Nagoya University, Chikusa-ku, Nagoya, Japan

(Received 10 September 1982; accepted 22 November 1982)

Abstract

The extinction factor η was numerically calculated for spherical crystals based on the new statistical dynamical theory [Kato (1976). *Acta Cryst.* **A32**, 458–466]. The optical paths in the Bragg case and other geometrical cases such as the Laue–Bragg–Laue are properly treated, so that the accuracy is estimated to be 0.1% for $\mu_0 R \leq 3.0$, $\sigma R \leq 2.0$ and $\theta_B \leq 30^\circ$ (μ_0 absorption coefficient, σ the coupling constant of the energy transfer equations, θ_B the Bragg angle). Based on these calculations a universal fitting function $\eta(\mu_0 R, \sigma R, \theta_B)$ is proposed in the above-mentioned domains. The accuracy is better than 0.4% if η is larger than 10%. The difference between the present and the conventional theories is significant if the extinction exceeds 20%.

1. Introduction

One of the authors has proposed a new theory on secondary extinction (Kato, 1976, 1979, 1980, 1982). The present paper is written for two purposes. The first is to calculate numerically the extinction factor for spherical crystals, which are often used for accurate determination of crystal structures. So far, the calculation has been made only for parallel-sided crystals (Kato, 1980), for simplicity. For finite crystals like a cylinder and a sphere, the application of the simplest solution of the energy transfer equations in the Laue cases is insufficient to obtain the diffracted intensity for the whole crystal, because the optical paths in the Bragg cases and other geometrical cases are involved.

In the present calculation, the correction is made approximately by using the rigorous solutions available for trapezoidal crystals. Not only the numerical values for a discrete set of parameters $\mu_0 R$, σR and θ_B , but also an analytical fitting function will be presented. Here, R is the radius of the crystal and σ is the coupling constant of the basic energy transfer equations. μ_0 and θ_B are the normal absorption coefficient and the Bragg angle, respectively. So far, to our knowledge, no such universal function has been presented.

The second aim is to illustrate the numerical difference between the conventional and present theories. Again, so far, it has been demonstrated only for parallel-sided crystals (Kato, 1982). Then, a significant discrepancy of more than 10% was noticed when the extinction factor was less than about 25%. A similar result is obtained here for spherical crystals.

2. The theoretical basis

In order to obtain the fundamental equation to describe secondary extinction the following energy transfer equations (ETE) are assumed (Kato, 1976).

$$\frac{\partial I_0}{\partial s_0} = -\mu_e I_0 + \sigma I_g \quad (1a)$$

$$\frac{\partial I_g}{\partial s_g} = -\mu_e I_g + \sigma I_0, \quad (1b)$$

where I_0 and I_g are the total intensities carried by the direct (O) and Bragg-reflected (G) beams. They